Studies on the mechanisms for posttranscriptional regulation of gene expression of Friend murine leukemia virus

転写後調節を介したマウス白血病ウイルス遺伝子の発現制御機構に関する研究

11D5606　待永明仁　　　指導教授　高瀬明

SYNOPSIS

マウス白血病ウイルス(MLV)の遺伝子は、5'LTR (long terminal repeat) に続いて、5'リーダー配列、*gag*、*pol*、*env*、及び、3'LTR が並ぶ構造をしている。5'スプライス部位は5'リーダー配列内に、3'スプライス部位は*pol*遺伝子内に存在している。宿主細胞のDNA に組み込まれたウイルス DNA からは、全長の mRNA、及び、スプライシングを受けた *env*-mRNA の 2 種類の mRNA が生成される。全長の mRNA からは Gag、及び、Pol タンパク質が、*env*-mRNA からはウイルス表面タンパク質 Env が翻訳される。MLV は、ウイルス遺伝子の発現を調節するアクセサリータンパク質を有しておらず、ウイルスの遺伝子発現制御機構については不明な点が多い。これまでの当研究室の研究により、*env*-mRNA は、スプライシングの過程を経ることで安定性を獲得し、Env タンパク質が効率的に翻訳されることが明らかとなった。さらに、*gag* 遺伝子内の *Hind*III-*Bgl*II 領域(878-1904 nt)にスプライシングの制御に関わるエレメントが含まれることが示された。これらの背景に基づき、本研究は、スプライシングを介した MLV の遺伝子発現機構の解析、及び、*gag* 遺伝子内に存在するスプライシング制御エレメントの同定と機能解析を行った。最初に、スプライスされた *env*-mRNA、及び、スプライスされない *env*-mRNA を産生するベクターを用いて、MLV のスプライシングが、*env*-mRNA の 3' 末端プロセシング、及び、*env*-mRNA のポリソーム構造形成に与える影響について解析した。その結果、スプライシングを受けた *env*-mRNA は正常に poly(A)鎖が付加されていたが、スプライシングを受けない *env*-mRNA の一部にポリアデニル化が不完全な mRNA が検出された。また、スプライシングを受けた *env*-mRNA の 69%がポリソーム構造をとっていたが、スプライシングを受けない *env*-mRNA では、ポリソーム構造をとっている mRNA は 24%であった。これらの現象は、*env* 遺伝子を *luciferase* 遺伝子に置換したベクターでは見られなかった。次に、*Hind*III-*Bgl*II 領域を段階的に欠失させた種々のベクターを用いて、スプライシング制御に関わるシスエレメントの解析を行った。その結果、*gag*領域内の 38nt 断片(1612-1649nt)に、正しいスプライス部位が選択されるために必須なエレメントが含まれることが明らかとなった。また、38nt 断片の上流領域(1183-1611nt)には、スプライス部位の選択に、正または負に影響を及ぼすエレメントが存在することが示された。さらに、38nt 断片は、3'スプライス部位の上流に存在する *Sph*I-*Nde*I 領域(5140-5400nt)と相互作用することにより、機能することも明らかとなった。本研究により、*env*-mRNA は、スプライシングを受けることにより、3' 末端のポリアデニル化の効率、及び、ポリソーム構造の形成効率が、*env* 遺伝子依存的に促進されることが示された。 さらに、MLV のスプライス部位の選択に正に作用する 38nt 新規シスエレメントが明らかにされた。

Keywords: Friend murine leukemia virus, gene expression, posttranscriptional regulation, splicing, polyadenylation, polysome

1. Introduction

The genome of murine leukemia virus (MLV), which belongs to the simple retrovirus family, contains a 5'LTR, a 5' leader sequence, *gag*, *pol*, *env*, and a 3'LTR. The *gag* gene encodes the structural proteins of the virion and the *pol* gene encodes a protease, reverse transcriptase and integrase. The *env* gene encodes the Env protein, which has a surface domain (SU) and a transmembrane domain (TM). There is a 5' splice site (5'ss) in the 5' leader sequence of the *gag* gene and a 3' splice site (3'ss) in the 3' end of the *pol* gene. Both full-length unspliced and spliced mRNAs are produced in MLV-infected cells. Gag and Pol proteins are translated from unspliced mRNAs and the Env protein is translated from spliced mRNA(1). The Env protein of MLV plays important roles not only in viral adsorption to cells but also in the induction of neuropathogenic disease following infection by the virus (2). In previous studies, we showed that the level of Env expression in neuropathogenic A8-MLV is correlated with neuropathogenicity (3, 4). Thus, elucidation of the regulatory mechanisms for production of *env*-mRNA will be important for understanding the functions of the Env protein. MLV and other simple retroviruses have no regulatory genes, such as those that control gene expression, including splicing events, in lentiviruses. We previously found that splicing is important for increasing *env*-mRNA stability and translation(5). However, the detailed mechanism for gene expression of MLV due to splicing is still not clear. We have also shown that the positive and negative regulatory regions within the intron that controls Env expression in Friend MLV at the level of *env*-mRNA expression do so by controlling splicing efficiency(5). Overall, however, the molecular mechanisms that regulate splicing in MLV, including the selection of splice sites, are not well understood. In this thesis, we focused on splicing of MLV to understand mechanisms for posttranscriptional regulation of MLV gene expression. First, effects of splicing of Friend MLV *env*-mRNA on its 3' end processing and polysome structure formation were studied. Second, *cis*-elements within *gag* that regulate splicing were analyzed.

2. Materials and Methods

2.1 Cell culture and transfection

Hela cells were grown in Dulbecco's Modified Eagle's Medium - low glucose (Sigma-Aldrich) supplemented with 10% fetal calf serum (MP Biomedicals), 50 units penicillin (Gibco)/ml and 50 μg streptomycin (Gibco)/ml, at 37°C in 5% CO_2. NIH3T3 cells were grown using the same conditions as Hela cells except NIH3T3 cells were incubated in 7% CO_2. The cells (1×10^6 cells) were transfected the next day with 8 μg viral expression vectors using Lipofectamine 2000 Reagent (Invitrogen) diluted with Opti MEM (Invitrogen) according to the manufacturer's instructions.

2.2 Determination of poly(A) tail length

Hela cells were transfected with vectors and total RNA was extracted 24 h post-transfection using an RNeasy Mini Kit (QIAGEN) according to the manufacturer's instructions. After treatment with RNase-free DNase (QIAGEN), 4 μg RNA was added to each ligation reaction. The anchor primer oligo1 (5'-GGGACAGCCTATTTTGCTAG-3') was ligated to the 3' end of the RNA and reverse transcription (RT) then was carried out using the poly(dT)+oligo2 primer (5'-CTAGCAAAATAGGCTGTCCCTTTTTTTTTT-3'). Nested PCR was carried out to amplify the viral mRNA poly(A) tail. In

the first PCR, a forward oligo3 primer targeting the 3' end of U3 in the 3' LTR (5'-GCCCTATAAAAGAGCTCACAACC-3') and a reverse oligo2 primer (5'-CTAGCAAAATAGGCTGTCCC-3'), which is complementary to the oligo1 sequence, were used. After purification of the first PCR products using a MicroElute Clean-Up Column (FAVORGEN), a second PCR was performed. In the second PCR, a forward oligo4 primer targeting the 5' end of the R region in the 3' LTR (5'-AGTCCTCCGACAGACTGAGT-3') and a reverse oligo5 primer targeting the 3' end of the oligo2 and poly(dT) sequence (5'-AAAATAGGCTGTCCCTTTTT-3') were used. The resulting PCR products were separated by electrophoresis on a 5% polyacrylamide gel in TBE buffer and stained with ethidium bromide.

2.3 Quantitation of *env*-mRNA, total viral RNA, and *gapdh*-mRNA by real-time RT-PCR

To evaluate the copy numbers of cDNAs from *env*-mRNA in the RT reaction products after RT synthesis using the poly(dT)+oligo2 primer, quantitative real-time PCR was performed. Briefly, the primers and probe used to quantitate cDNA of *env*-mRNA were forward s1-primer (5'-GAGACCCTTGCCCAGGGA-3'), reverse s2-primer (5'-TGCCGCCAACGGTCTCC-3'), and TaqMan ss-probe (5'-CACCACCGGGAGCTCATTTACAGGCAC-3'). The primers and probe used to quantitate cDNA corresponding to total RNA from the m1 and splA8 vectors were forward e1-primer (5'-AGGACCTCGGGTCCCAATAG-3'), reverse e2-primer (5'-TTAGGTAGCGGGAACGAAAGTT-3'), and TaqMan e-probe (5'-CCGAACCCCGTCCTGGCAGAC-3'). To quantitate *gapdh*-mRNA, TaqMan Human Control Reagents containing primer sets and probe (Applied Biosystems) were used.

2.4 Fractionation of cell lysates by sucrose density gradient centrifugation

Polysome fractions were obtained by fractionation of cell extracts by sucrose density gradient centrifugation. Briefly, transfected or infected NIH3T3 cells (6×10^6) were incubated in medium containing 100 μg cycloheximide/ml for 15 min. The cells then were lysed in 1 ml hypotonic lysis buffer [1.5 mM KCl, 2.5 mM MgCl$_2$, 5 mM Tris-HCl (pH 7.4), 1% Triton X-100, 1% sodium deoxycholate, 100 μg cycloheximide/ml, 1 mM dithiothreitol, 100 units RNase inhibitor (TaKaRa)/ml]. After 10 min on ice, lysates were centrifuged at 10,000 x g for 10 min and the resulting cytosol-containing supernatant was removed and layered onto a 10-50% sucrose density gradient in buffer [80 mM NaCl, 5 mM MgCl$_2$, 20 mM Tris-HCl (pH 7.4), 1 mM dithiothreitol]. After ultracentrifugation at 30,000 rpm for 3 h at 4°C, 16 fractions were obtained. The RNA in each fraction was extracted using TRIzol LS Reagent (Invitrogen) and measured by absorbance at 260 nm.

2.5 Quantitation of *env*-mRNA in each fraction by real-time RT-PCR

Extracted RNA from each fraction was treated with RNase-free DNase (QIAGEN). Equal volume samples of each fraction were used as template for RT using an oligo(dT) primer (Invitrogen). In its volume of the fraction that had a largest absorbance peak at 260 nm, 2 μg RNA was contained. A portion of the resulting cDNA was amplified by real-time PCR using a 7500 Real-Time PCR System (Applied Biosystems). The primers and probe used to quantitate *env*-mRNA were s1-primer, s2-primer, and TaqMan ss-probe. To quantitate *gapdh*-mRNA, TaqMan Rodent Control Reagents containing primer sets and probe were used.

2.6 Construction of vector

To construct the d3 vectors *Aat*II and *Sph*I were used to carry out a restriction digest of m1. The enzyme sites were blunted using a DNA Blunting Kit (TaKaRa), after which blunt-end ligation was performed. To construct the d3+1026 vector, the *Hin*dIII–*Bgl*II fragment of m1 was cloned by PCR using a forward primer containing an *Aat*II restriction site in the 5′ terminus, and a reverse primer containing the *Sph*I restriction site in the 5′ terminus. The *Art*II–*Sph*I fragment was recombined using the restriction site of m1. The vectors, B1, B2, B3, B2-a, B2-b, B2-c, B3-d, B3-e, B3-f, B3-d1, B3-d2, B3-d3, and B3-d4, which have serially truncated *Hin*dIII-*Bgl*II regions of m1, were constructed using a KOD-Plus-Mutagenesis Kit (TOYOBO). To construct the B3-d4inv38 vector two-stage inverse PCR was performed using the 2 sets of primers. To construct the d4+1026 vectors, *Sph*I and *Nde*I were used to carry out a restriction digest of d3+1026. The enzyme sites were blunted using a DNA Blunting Kit, after which blunt-end ligation was performed.

2.7 RT-PCR analysis of viral spliced mRNA in transcripts

Total cellular RNA was isolated from transfected cells using RNeasy Mini Kit (QIAGEN) according to the manufacturer's instructions. After treatment with RNase-free DNase (QIAGEN), 2 μg of RNA were added to the RT reaction, which used an oligo (dT) primer (Invitrogen). The spliced mRNA was detected by PCR using Go Taq (Promega) and specific s1 and s2 primers. PCR products were separated on 2% agarose gels in TBE buffer and stained with ethidium bromide.

3. Results and Discussion
3.1 Effects of splicing on the polyadenylation of *env*-mRNA

The m1 vector carried the full-length A8-MLV provirus genome and generated spliced *env*-mRNA (Fig. 1A). Electrophoretic analysis of the products of nested PCR showed a smear in the 100-200 bp range in the mRNA from samples obtained from m1-transfected cells (lane 1 of Fig. 1B). Sequence analysis showed that these smears contained multiple A nucleotides 11-21 nt downstream of the poly(A) addition signal (AAUAAA). To examine whether *env*-mRNA splicing affected polyadenylation of the mRNA, the poly(A) tail length of spliced *env*-mRNA and unspliced *env*-mRNA were compared using the m1 and splA8 vectors (Fig. 1A). The splA8 vector was designed to generate unspliced *env*-mRNA by deletion of the intron region in m1. Electrophoretic analysis of the nested PCR products showed a smear in the 100-200 bp range for mRNA obtained from splA8-transfected cells (lane 3 of Fig. 1B). Sequence analysis showed that these smears contained multiple A nucleotides 11-21 nt downstream of the poly(A) addition signal (AAUAAA). Interestingly, an approximately 70 bp band was also detected in RNA from splA8-transfected cells. Sequence analysis showed that this band came from mRNA in which 5-8 A nucleotides were attached just downstream of the poly(A) addition signal and the oligo1 sequence (Fig. 1B). This band was not observed in m1-transfected cells, as shown in lane 1 of Figure 1B. In this experimental system, the length of the mRNA poly(A) tail could be determined in both unspliced full-length MLV mRNA and in spliced *env*-mRNA from m1-transfected cells. Therefore, to confirm that the first strand of cDNA synthesized by RT using the poly(dT)+oligo2 primer contained *env*-mRNA, PCR was performed using s1 and s2 primers. These primers were designed to amplify the 94 bp fragment containing the splicing junction region in the cDNA from *env*-mRNA. As shown in Figure 1C, 94 bp bands were detected in cDNA of *env*-mRNA from m1- and splA8-transfected cells. All 94 bp bands were confirmed to come from *env*-mRNA by sequence analysis (data not shown). In addition, the copy number of cDNA synthesized from *env*-mRNA was evaluated by quantitative

real-time PCR. The copy number of cDNA from splA8 *env*-mRNA was 5.3-fold more than that synthesized from m1 *env*-mRNA (Fig. 1D). The copy number of cDNA synthesized from total viral RNA was also evaluated by quantitative real-time PCR, and it was not significantly different from results obtained for RNA from m1- and splA8-transfected cells. The transfection efficiency, which was measured by the copy number of plasmid DNA in transfected cells, was not significantly different in m1- and splA8-transfected cells. To confirm the finding that the approximately 70 bp band was detected only in splA8-transfected cells that contained unspliced *env*-mRNA but not in m1-transfected cells that contained spliced *env*-mRNA, the amount of template cDNA for the 1st PCR was normalized by the amount of cDNA synthesized from *env*-mRNA; the volume of the RT reaction mixture containing m1 cDNA used as a template for the first PCR was 5.3 times that of the RT reaction mixture containing splA8 cDNA. The nested PCR reactions produced a smear in the 100-200 bp range for mRNA from m1-transfected cells, but the approximately 70 bp band was not detected (lane 2 of Fig. 1B). There were no differences in the poly(A) tail smear patterns of the *gapdh*-mRNAs from all samples (data not shown). The data presented herein suggest that splicing of MLV plays an important role in complete polyadenylation of *env*-mRNA. Interestingly, when the *env* gene in m1 and splA8 was replaced by the *luciferase* (*luc*) gene, splicing did not affect the 3' end structure of *luc*-mRNA (data not shown). These data suggested that there were positive *cis*-elements within the *env* region to complete the polyadenylation of *env*-mRNA by splicing.

3.2 Effects of splicing on formation of *env*-mRNA polysome structures

Formation of polysome structures of mRNA is generally correlated with mRNA translation efficiency. To investigate whether splicing of MLV affected formation of *env*-mRNA polysome structures, we used the m1 and splA8 vectors to compare the amount of *env*-mRNA associated with polysome structures in spliced and unspliced *env*-mRNA. Lysates of NIH3T3 cells transfected with m1 or splA8 were separated by centrifugation on linear 10–50% sucrose density gradients. After extraction of RNA from each fraction, the distribution of total RNA and ribosomal RNA (rRNA) was analyzed by measurement of absorbance at 260 nm and agarose gel electrophoresis, respectively (Fig. 2). mRNA in polysome structures was found in higher density fractions, while mRNA that was not in polysome structures was in lower density fractions. In lysates of m1-transfected cells, there was a large absorbance peak at 260 nm in fractions 6-9 (Fig. 2A). Agarose gel electrophoresis analysis showed that these fractions contained most of the 28S and 18S rRNAs in the lysate. There were small peaks at 260 nm in higher density fractions 11-16. These fractions also contained 28S and 18S rRNA, in agreement with these fractions containing polysomes. As a control, the distribution of *gapdh*-mRNA was examined by real-time RT-PCR. There were two peaks of *gapdh*-mRNA, one in lower density fraction 8 and the other in higher density fractions 13-15 (Fig. 2A). The distribution of *env*-mRNA was examined by real-time RT-PCR. As shown in Fig. 2A, most *env*-mRNA was in fractions 13-16, which were polysome fractions. From quantitative analysis of these real-time PCR results, 69% of *env*-mRNA in m1-transfected cells was in the polysome structures in fractions 11-16. A similar experimental analysis of lysates of splA8-transfected cells showed that a large amount of *env*-mRNA was in fractions1-8(Fig. 2B). Although 24% of *env*-mRNA in splA8-transfected cells was in polysome structures (fractions 10-16), this was significantly less (p<0.01) than the 69% in polysome structures in m1-transfected cells. In A8-MLV infected
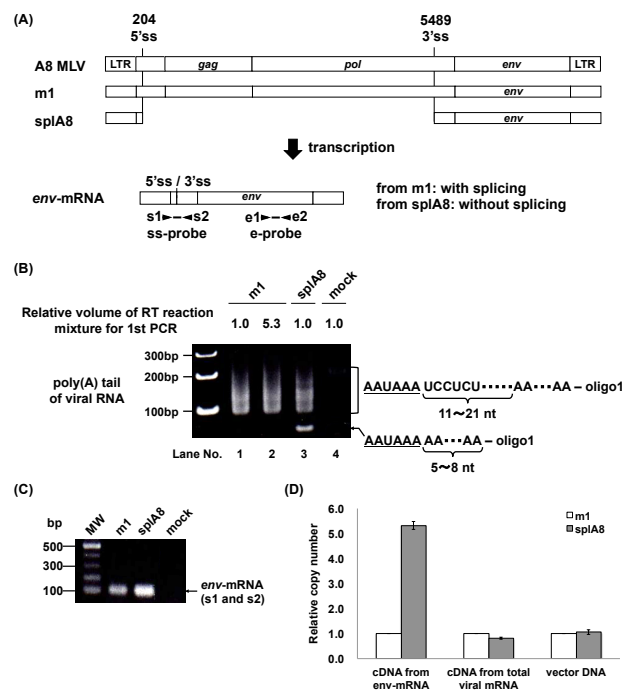

Fig. 1 (A) Structure of the MLV provirus genome and vectors in this study, and *env*-mRNA. **(B)** Determination of poly(A) tail length of mRNA from m1- and splA8-transfected cells. **(C)** Detection of cDNA synthesized from *env*-mRNA obtained from m1- and splA8-transfected cells with a poly(dT)+oligo2 primer. **(D)** Measurement of the copy number of cDNA synthesized from *env*-mRNA and total viral RNA and the copy number of vector DNA in m1- and splA8-transfected cells by real-time PCR.

cells (Fig. 2C), 61% of *env*-mRNA was in polysome structures (fractions 11-16), which was not significantly different from the 69% in polysome structures in m1-transfected cells. The results showed that the fraction of spliced *env*-mRNA in polysome structures was significantly greater than of unspliced *env*-mRNA. This indicated that splicing promoted the formation of *env*-mRNA polysome structures. Interestingly, when the *env* gene in m1 and splA8 was replaced by the *luc* gene, splicing did not affect polysome structure formation of *luc*-mRNA and the degree of polysome structure formation of unspliced *luc*-mRNA was higher than that of unspliced *env*-mRNA (data not shown). Thus, it was suggested that there were *cis*-elements within the *env* region that contribute to polysome structure formation of mRNA.
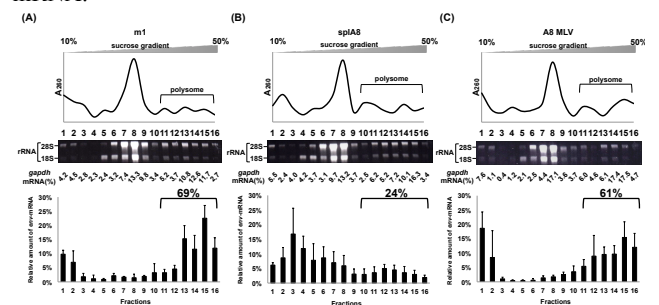

Fig. 2 Polysome profiles of cells transfected with **(A)** m1 and **(B)** splA8, or infected with **(C)** MLV.

3.3 Narrowing down the region within the *Hind*III-*Bgl*II fragment (879-1904 bp) that is crucial for splicing at the correct 5'ss and 3'ss

We found that when the *Hind*III–*Bgl*II fragment was deleted from the m1 vector (B vector), there were abundant splice

variants among the transcripts (5). We transfected the m1 vector into NIH3T3 cells and examined generation of spliced mRNA after 48 hr by RT-PCR using the s1 and s2 primers (Fig. 3). As shown in Figure 3, we detected the 94 bp band in the transcripts of m1. In contrast, in the transcripts of the B vector, we detected a band of approximately 300 bp (Fig. 3). We used the d3 vector to analyze the importance of the *Hin*dIII–*Bgl*II fragment in splicing, in which the majority of the intronic *Aat*II–*Sph*I (366–5139 bp) fragment has been deleted from m1. The d3 vector yielded the splice variant and unspliced transcripts (Fig. 3). When we inserted the *Hin*dIII–*Bgl*II fragment between 366 and 5139 bp of the d3 vector (to produce the d3+1026 vector), we only produced correctly spliced mRNA (Fig. 3).

We first sought to narrow down the region within the *Hin*dIII–*Bgl*II fragment that is crucial for splicing at the correct 5′ss and 3′ss of Fr-MLV. To this end, we constructed B1, B2, and B3 vectors with serially truncated *Hin*dIII–*Bgl*II fragments from the entire sequence of m1. Among these vectors, B2 and B3 yielded a small amount of mRNA splice variants in addition to correctly spliced mRNA (Fig. 3). We sought to further narrow down the 1183–1904 bp region by constructing the B2-a to B3-f vectors that are serially truncated in this region. The transcripts of the B2-a, B2-b and B2-f vectors included only correctly spliced mRNA. The transcripts of the B2-c and B3-e vectors included abundant correctly spliced mRNA and a few mRNA splice variants. It is noteworthy that B3-d included only mRNA splice variants. To further narrow down the 1542–1649 bp fragment, we next constructed the B3-d1 to B3-d4 vectors that were serially truncated in the fragment. In B3-d1, the transcripts contained normally spliced mRNA and a few mRNA splice variants. In B3-d2 and B3-d3, the transcripts contained only correctly spliced mRNA and we detected no splice variants. Interestingly, B3-d4, in which the 1612-1649 bp fragment was deleted from m1, only yielded mRNA splice variants. The transcripts from the B3-d4inv38 vector carrying a reverse sequence of the 1612-1649 bp fragment included only splice variants. These findings showed that the 38 nt region (1612–1649 nt) contains the important elements that regulate splicing at the correct 5′ss and 3′ss. Further analyses of a series of vectors carrying the 38 bp fragment and its flanking sequences showed that a region (1183–1611 nt) upstream of the 38 nt fragment also contains sequences that positively or negatively influence splicing at the correct splice sites (data not shown).

3.4 Effect of the upstream region of 3'ss of MLV on fraction of the 38 nt fragment and its flanking sequence

In a previous study, we showed that the *Sph*I–*Nde*I fragment located approximately 100 nt upstream of the 3'ss could influence splicing efficiency and the appearance of splice variants (5). Interestingly, the structure of the splice variant was identical to that of a splice variant observed in the transcripts of B3−d4 (Fig. 3). The vectors developed for the experiments shown in Figure 3 contain the *Sph*I–*Nde*I region. To examine whether this region influenced control of splicing by the 38 nt fragment and its flanking sequence, as shown in Figure 4, we deleted it from d3+1026 (Fig. 3); the resulting transcripts were correctly spliced. By contrast, we obtained abundant splice variants from the transcripts of d4+1026 (Fig. 4). The findings show that a synergistic interaction between the 5140– 5400 nt region located in the upstream region of the 3'ss and the 38 nt fragment and its flanking sequence is required for splicing at the correct 5′ss and 3′ss.

4. Conclusion

In this thesis, we focused on splicing to understand mechanisms for posttranscriptional regulation of gene expression of MLV. It was showed that splicing of MLV promoted the
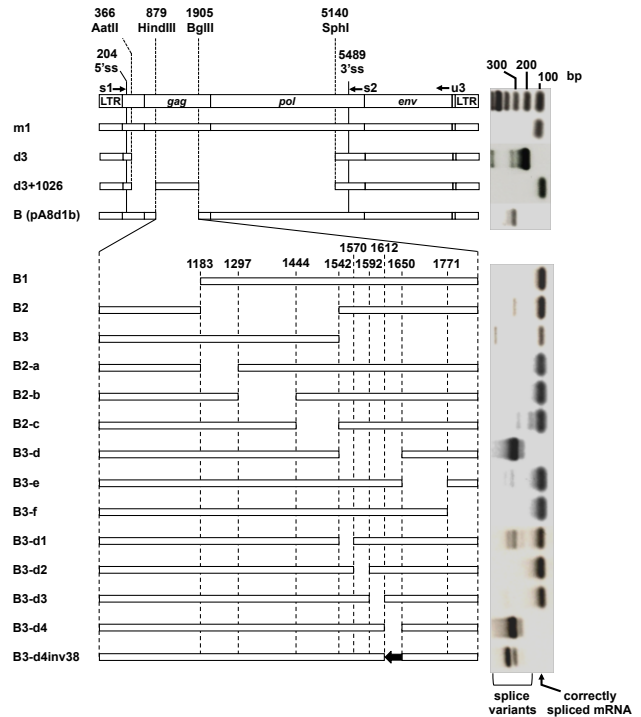

Fig. 3 Structures of d3, d3+1026 and vectors with a serially truncated *Hin*dIII–*Bgl*II fragment of m1 and detection of the splice junction region of *env*-mRNA in the transcripts of vectros.
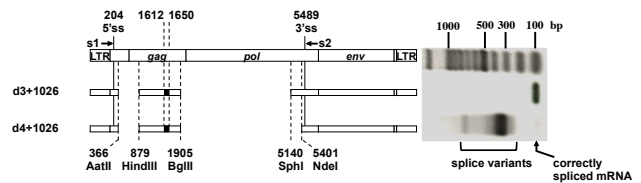

Fig. 4 Structures of d4+1026 vector and detection of the splice junction region of *env*-mRNA in the transcripts of the vectors.

efficiency of complete polyadenylation of *env*-mRNA and the formation of *env*-mRNA polysome structures. These splicing-dependent phenomena were not observed with expression vectors in which the *env* gene was replaced by the *luc* gene. In addition, it was indicated that the 38 nt fragment within *gag* plays an important role in splicing at the correct 5′ss and 3′ss of MLV. It was also showed that a region (1183–1611 nt) upstream of the 38 nt fragment contains sequences that positively or negatively influence splicing at the correct splice sites. The 38 nt fragment appears to exert this function in cooperation with a region located just upstream of the 3'ss. To our knowledge, this is the first report showing new mechanisms for posttranscriptional regulation of gene expression of MLV, in which splicing of MLV promoted the efficiency of complete polyadenylation of *env*-mRNA and the formation of *env*-mRNA polysome structures in an *env* gene-dependent manner and the 5' and 3' splice sites of MLV are selected correctly through the function of the 38 nt region within *gag* gene.

5. References

1. Rabson A. B., et al. 1997. Retroviruses. Cold Spring Harbor Laboratory Press, pp.205-62.
2. Takase-Yoden, S., et al. 1997. Virology 233:411-422.
3. Takase-Yoden, S., et al. 2006. Microbiol. Immunol. 50:197-201.
4. Takase-Yoden, S., et al. 2005. Virology 336:1-10.
5. Yamamoto, N., et al. 2009. Virology 385:115-125.